ON MEASURING DOPPLER SHIFTS BETWEEN TAGS IN A BACKSCATTERING TAG-TO-TAG NETWORK WITH APPLICATIONS IN TRACKING

Abeer Ahmad,* Yuanfei Huang,** Xiao Sha,** Akshay Athalye,** Milutin Stanaćević,** Samir R. Das,* and Petar M. Djurić**

*Computer Science Stony Brook University Stony Brook, NY 11794 **Electrical and Computer Engineering Stony Brook University Stony Brook, NY 11794

ABSTRACT

In this paper, we present a technique whereby passive tags can track each other in a backscattering tag-to-tag network (BTTN). In such a network, passive tags without any on-board radio transceivers communicate directly with each other by backscattering an external excitation signal. First, we explain how the tags determine their distances to other communicating tags in their proximity and then how they can track nearby tags. Our technique is based on multiphase backscattering, more specifically, on the ability of backscattering tags to systematically change the phase offset of the signal that is being backscattered. A passive receiving tag with an envelope detector can then examine the received signal amplitude over the multiple backscattering phases and can draw inferences about the inter-tag distance. We demonstrate our method and show its accuracy on tags that we have built in our lab. Experiments show that our passive tags can measure Doppler shifts with approximately the same accuracy as that achieved by active conventional RFID readers. Our median tracking error based on data from two tags is only about 2.5 cm.

Index Terms— tag-to-tag communication, backscattering, tracking, Doppler shift

1. INTRODUCTION

The Radio Frequency IDentification (RFID) technology has continued to make strides in recent years, particularly vis-á-vis the ongoing advances in the Internet of Things (IoT). One of the most important tasks in the IoT apart from object identification is their precise localization and tracking [1, 2]. In classical RFID systems, a reader with an active radio provides a continuous wave (CW) signal and interrogates its environment for the presence of passive RFID tags. The reader is rather complex and intelligent and, as a result, able to process and interpret signals in challenging settings. The tags only communicate with the reader and they do it by simply reflecting the CW signal emitted by the reader. During the reflection, they modulate their antenna reflection coefficients by switching between two impedances that terminate the tag antenna circuit, which in turn inscribe information in the reflected signal [3, 4]. When the tags receive an RF signal from the reader with information, they decode it by using passive envelope detectors followed by comparators [3, 4]. When the tag is in the range of the reader, the received signal by the tag has a high modulation index and its demodulation is not challenging. By contrast, the backscattered signal from the tag that is

The authors are thankful for the support of NSF under Awards CNS-1901182 and CNS-1763843.

received by the reader has a much lower modulation index, and consequently is much more difficult for demodulation. The active reader however, is equipped with circuitry that implements IQ demodulation and active cancellation of the interfering carrier signal and can therefore read the information in the signals from the tags even if these signals are of poor quality. The use of RFID readers in the IoT paradigm, however, is not scalable due to their cost.

A very promising alternative to the classical system is Backscattering tag-to-tag networking or BTTN, which is a system without active RFID readers, where the tags can communicate among themselves directly, while still using the same principles of backscattering. In a tag-to-tag link, the Tx tag backscatters information by modulating either a CW signal emitted by a dedicated exciter or an ambient RF signal. The Rx tag receives a signal that is a combined superposition of the excitation signal and the Tx backscatter. This combined signal must be demodulated using the envelope detector of the Rx tag. In this communication scenario, the Rx tag must resolve a backscatter signal from another tag, which is typically a signal with much lower modulation index than that received from an RFID reader. This calls for a more elaborate design of the tag's demodulator circuit after the envelope detector [5].

More recently, we have developed backscattering tags that employ multiphase probing while they communicate with other tags. [6]. The probing allows the tags to explore the backscatter channel by reflecting the incident RF signal with different changes in the phase. The extracted channel information can be used for various purposes including activity recognition [7]. In this paper, we show how this information can be exploited for localization and tracking.

The most closely related work to ours is [8]. Here, the authors track RFID tags using active RFID readers and achieve a median of 6 cm of tracking accuracy in real environments. In [9], active RFID readers are also used but in combination with ultra-wideband (UWB) signals to remove any mutipath effects. Other papers where methods based on active RFID are investigated include [10, 11]. In [12], the idea of putting two tags on an object for better tracking is introduced and the obtained accuracy is of the order of a couple of centimeters. In other papers, like [13, 14], similar centimeter level tracking accuracies have been reported.

The main contribution of this paper is a method for Doppler shift measurements that is done entirely on passive tags, unlike in existing work. The method exploits the concept of multiphase probing and, from it, inferring information about changing distances between two communicating tags. We show that we can measure Doppler shifts on passive tags almost as accurately as with costly conventional RFID readers. With our experiments, we demonstrate that with two tags in an office environment the median tracking error

is 2.5cm. This is comparable to related work that requires the use of RFID readers. Since our tags are passive and thus can be very inexpensive, the localization and tracking now can become scalable operations. Given the importance of these operations in IoT systems, this will propel many new and interesting applications.

The paper is organized as follows. In the next section, we define the mathematical model and explain how two passive backscattering tags can employ multiphase probing to estimate the distance from each other and also measure the Doppler shift of a moving tag, which allows for tracking. In Section 3, we provide experimental results that demonstrate the accuracy of the proposed method. We follow with some discussion about the proposed approach in Section 4 and with concluding remarks in Section 5.

2. MATHEMATICAL MODEL

We explain the mathematical model by using Fig. 1 which shows an exciter E and two tags T_1 and T_2 separated by distances d_1 , d_2 , and d, respectively. We emphasize, once again, that unlike conventional active wireless communication, T_1 and T_2 do not have radio transceivers. Instead they transmit by backscattering and receive using envelope detection. The exciter emits a CW at all times, and one of the tags is backscattering the CW whereas the other tag is acting as a receiver. The signal at the receiving tag is a superposition of the exciter's signal and the backscattered signal of the transmitter.

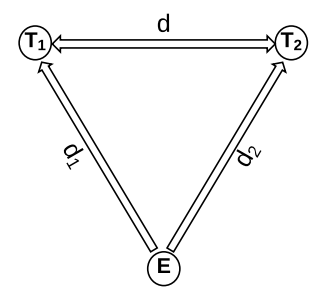


Fig. 1. A system overview with an exciter and two tags T_1 and T_2 that communicate directly.

2.1. The basic RF wave model

Suppose the exciter emits a sinusoidal signal with zero phase and frequency f_c . Then the phase of the propagated signal at a distance d is given by

$$\theta = \frac{2\pi d}{\lambda},\tag{1}$$

where $\lambda = c/f_c$, and c is the speed of light.

In Fig. 1, the phasor of the signal coming directly from the exciter to T_1 can be represented as

$$e_1 = a_{e_1} e^{j\theta_{e_1}},\tag{2}$$

where a_{e_1} is the amplitude of the signal, and θ_{e_1} is the difference between the phases of the CW at the exciter and that at T_1 , i.e., $\theta_{e_1} = (2\pi d_1)/\lambda$. Let the tag T_2 reflect the exciter signal with an additional phase ψ_2 , which depends on the impedance that is connected to the antenna. Then the phasor of the signal that comes from T_2 and is received by T_1 is given by

$$\tau_1 = a_{\tau_1} e^{j(\theta_{e_2} + \psi_2 + \theta_{\tau})},\tag{3}$$

where a_{τ_1} is the amplitude of the received signal from T_2 , θ_{e_2} is the difference between the phases of the CW at the exciter and that at T_2 and which is given by $\theta_{e_2} = (2\pi d_2)/\lambda$, and $\theta_{\tau} = (2\pi d)/\lambda$ is the phase difference due to the distance d between T_1 and T_2 . Thus, the overall signal at T_1 is the sum of the phasors from (2) and (3), i.e.,

$$s_1 = a_{e_1} e^{j\theta_{e_1}} + a_{\tau_1} e^{j(\theta_{e_2} + \psi_2 + \theta_{\tau})}.$$
 (4)

Our tags are passive, and they can only process the envelopes of signals (the amplitudes of the phasors). The square of the amplitude of s_1 in (4) is given by

$$|s_1|^2 = a_{e_1}^2 + a_{\tau_1}^2 + 2a_{e_1}a_{\tau_1}\cos(\theta_{e_1} - (\theta_{e_2} + \psi_2 + \theta_{\tau})).$$
 (5)

If the roles of the tags T_1 and T_2 are switched, we obtain for the square of the amplitude of s_2 (where s_2 is a phasor which is a sum of $e_2=a_{e_2}e^{j\theta_{e_2}}$ and $\tau_2=a_{\tau_2}e^{j(\theta_{e_1}+\psi_1+\theta_{\tau})}$) by

$$|s_2|^2 = a_{e_2}^2 + a_{\tau_2}^2 + 2a_{e_2}a_{\tau_2}\cos(\theta_{e_2} - (\theta_{e_1} + \psi_1 + \theta_{\tau})).$$
 (6)

The multiphase probing technique that we mentioned earlier refers to the ability of the tags to change the values of the phases ψ_1 (tag T_1) and ψ_2 (tag T_2). We explain how this plays an important role in the application of tracking of tags by way of measuring Doppler shifts

2.2. Measuring distance and Doppler shifts between two tags

First we show how the two tags can estimate the distance d between them. Assume that each tag can reflect at k different phases, where $k \geq 3$. We denote these phases by φ_n , $n \in \{1, 2, 3, \cdots, k\}$. Further, we assume that tag T_1 receives and tag T_2 reflects and that T_2 changes its phase in time according to

$$\psi_2(t) = \begin{cases} \varphi_n, & (n-1)T_s \le t < nT_s, \\ 0, & \text{otherwise,} \end{cases}$$
 (7)

where T_s is the period between two changes of the phase. Suppose next that the tag samples the envelope once per time period T_s . This entails that after sampling the envelope during each of the time periods (one sample per period), the tag has k samples of the form

$$|s_1[n]| = \sqrt{a_{e_1}^2 + a_{\tau_1}^2 + 2a_{e_1}a_{\tau_1}\cos(\theta_{e_1} - (\theta_{e_2} + \varphi_n + \theta_\tau))},$$
(8)

where $n \in \{1, 2, 3, \dots, k\}$. We rewrite (8) as

$$|s_1[n]| = \sqrt{\alpha_1 + \beta_1 \cos(\varphi_n - \gamma_1)}, \tag{9}$$

where

$$\alpha_1 = a_{e_1}^2 + a_{\tau_1}^2$$
; $\beta_1 = 2a_{e_1}a_{\tau_1}$; $\gamma_1 = \theta_{e_2} + \theta_{\tau} - \theta_{e_1}$. (10)

We note that the samples of $|s_1[n]|^2$ represent a sinusoid as a function of φ_n . When we know the values of φ_n , we can readily estimate the parameters of α_1 , β_1 and γ_1 . There is information about the distance between the tags in γ_1 , and more specifically in θ_τ . However, the estimation of d would require knowledge of θ_{e_1} and θ_{e_2} , which amounts to knowing the distances d_1 and d_2 . We observe, however, that when the roles of the tags are reversed (T_1 backscatters and T_2 receives), we have the parameter γ_2 at T_2 , which is given by

$$\gamma_2 = \theta_{e_1} + \theta_{\tau} - \theta_{e_2}. \tag{11}$$

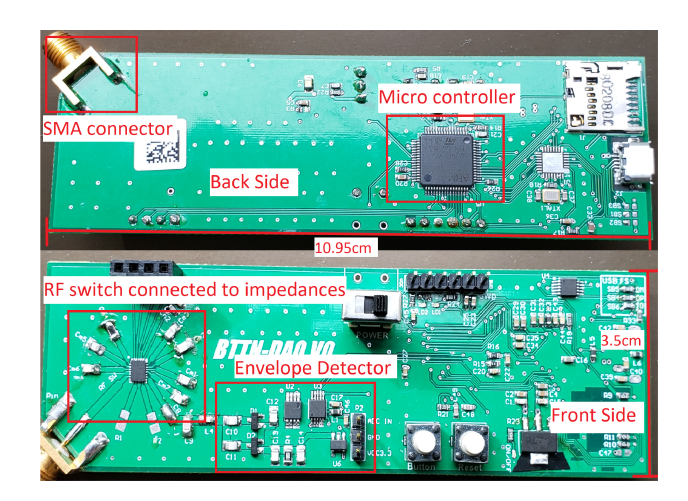


Fig. 2. Tag design.

From equations (10) and (11), we obtain

$$\gamma = \gamma_1 + \gamma_2
= \frac{4\pi d}{\lambda}.$$
(12)

Hence, from the estimated values of γ_1 and γ_2 (obtained from the sequences $|s_1[n]|^2$ and $|s_2[n]|^2$, $n \in \{1, 2, \cdots, k\}$), respectively, we can determine the distance between the tags T_1 and T_2 .

Next, we consider the case when one of the tags is backscattering and the other, the receiving tag, is moving toward the backscattering tag with a uniform velocity v. As a result, there is a Doppler shift in the received signal due to the continuous change in distance between the tags. For simplicity, let the distance between the tags at t=0 be d_0 . Then the instantaneous distance between the tags is $d(t)=d_0-vt$, and thus by using (12), we obtain

$$\gamma(t) = \frac{2\pi(d_0 - vt)}{\lambda}.$$
 (13)

This means that from two estimates of $\gamma(t)$ (at two different time instants), we can easily estimate the velocity of the moving tag v.

2.3. Processing of the data on the tag

Here we explain how the tags can estimate the parameters γ_i in (10) and (11). Basically, the tags have k measurements of the type

$$|s_i[n]|^2 = \alpha_i + \beta_i \cos(\varphi_n - \gamma_i), \quad n = 1, 2, \dots, k, \quad i = 1, 2.$$
 (14)

On the right-hand side of the above equation, the unknowns are α_i , β_i and γ_i out of which only γ_i is of interest. By simply forming the differences

$$\Delta_{n,i} = |s_i[n]|^2 - |s_i[n-1]|^2, \quad n = 2, 3, \dots k,$$
 (15)

where

$$\Delta_{n,i} = -2\beta_i \sin\left(\frac{\varphi_n + \varphi_{n-1}}{2} + \gamma_i\right) \sin\left(\frac{\varphi_n - \varphi_{n-1}}{2}\right), \quad (16)$$

with the nuisance parameter α_i being removed, the last equation can readily be transformed by elementary operations to a set of linear equations of the form

$$z_{n,i} = \rho_{n,i}\phi_{1,i} + \widetilde{\rho}_{n,i}\phi_{2,i}, \quad n = 2, 3, \dots, k,$$
 (17)

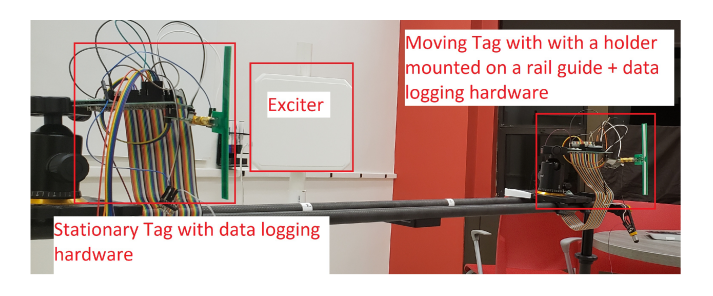


Fig. 3. System overview.

where

$$z_{n,i} = -\frac{\Delta_{n,i}}{2\sin\left(\frac{\varphi_n - \varphi_{n-1}}{2}\right)},$$

$$\rho_{n,i} = \sin\left(\frac{\varphi_n + \varphi_{n-1}}{2}\right), \quad \widetilde{\rho}_{n,i} = \cos\left(\frac{\varphi_n + \varphi_{n-1}}{2}\right),$$

$$\phi_{1,i} = \beta_i \cos \gamma_i, \quad \phi_{2,i} = \beta_i \sin \gamma_i,$$

where the $z_{n,i}$ s, $\rho_{n,i}$ s, and $\widetilde{\rho}_{n,i}$ s are all known. The system of equations (17) is linear, and the tag can readily obtain the estimates of the unknown parameters $\phi_{1,i}$ and $\phi_{2,i}$. Once these parameters are estimated, the unknown γ_i can easily be obtained from them. We note that with the above approach, the tags do not have to use phases that are uniformly separated.

3. EXPERIMENTAL EVALUATIONS

For experimental demonstration, a prototype RF tag has been designed and fabricated. This tag has a multi-phase modulator and demodulator, which is a passive envelope detector. The tag connects to a custom made dipole antenna tuned to 915 MHz, which is in the middle of the UHF ISM spectrum. The modulator comprises an RF switch that connects one of the k phases to the antenna The selection logic is implemented on a low-power microcontroller stm32f205ret. The impedances are preselected to provide specific reflection phases. The phase values almost uniformly cover the range from 0 to 360 degrees. In the demodulator design, the output voltage of the envelope detector is recorded using a 16 bit ADC which can sample at a rate of 860 samples per second. Figure 2 shows the prototype of the tags.

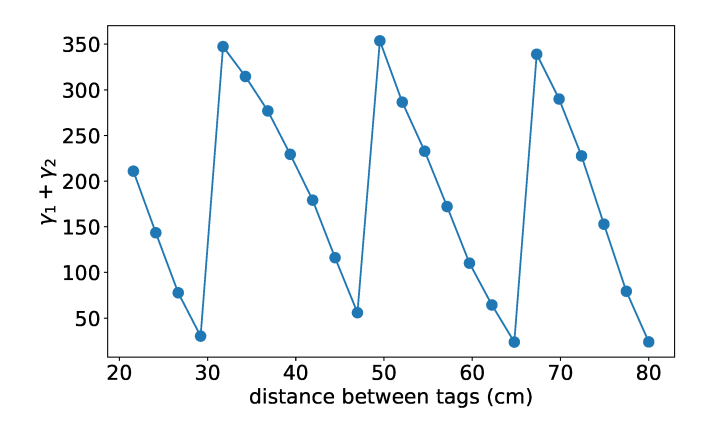


Fig. 4. Change of the channel phase with distance.

We used a CW generator at 915 MHz connected to a circularly polarized panel antenna as excitation source. The exciter is set to a

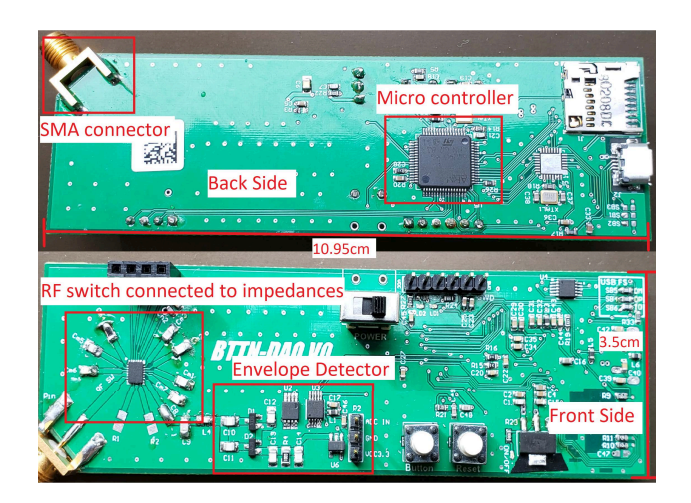


Fig. 2. Tag design.

From equations (10) and (11), we obtain

$$\gamma = \gamma_1 + \gamma_2
= \frac{4\pi d}{\lambda}.$$
(12)

Hence, from the estimated values of γ_1 and γ_2 (obtained from the sequences $|s_1[n]|^2$ and $|s_2[n]|^2$, $n \in \{1, 2, \dots, k\}$), respectively, we can determine the distance between the tags T_1 and T_2 .

Next, we consider the case when one of the tags is backscattering and the other, the receiving tag, is moving toward the backscattering tag with a uniform velocity v. As a result, there is a Doppler shift in the received signal due to the continuous change in distance between the tags. For simplicity, let the distance between the tags at t=0 be d_0 . Then the instantaneous distance between the tags is $d(t)=d_0-vt$, and thus by using (12), we obtain

$$\gamma(t) = \frac{2\pi(d_0 - vt)}{\lambda}.$$
 (13)

This means that from two estimates of $\gamma(t)$ (at two different time instants), we can easily estimate the velocity of the moving tag v.

2.3. Processing of the data on the tag

Here we explain how the tags can estimate the parameters γ_i in (10) and (11). Basically, the tags have k measurements of the type

$$|s_i[n]|^2 = \alpha_i + \beta_i \cos(\varphi_n - \gamma_i), \quad n = 1, 2, \dots, k, \quad i = 1, 2.$$
 (14)

On the right-hand side of the above equation, the unknowns are α_i , β_i and γ_i out of which only γ_i is of interest. By simply forming the differences

$$\Delta_{n,i} = |s_i[n]|^2 - |s_i[n-1]|^2, \quad n = 2, 3, \dots k,$$
 (15)

where

$$\Delta_{n,i} = -2\beta_i \sin\left(\frac{\varphi_n + \varphi_{n-1}}{2} + \gamma_i\right) \sin\left(\frac{\varphi_n - \varphi_{n-1}}{2}\right), \quad (16)$$

with the nuisance parameter α_i being removed, the last equation can readily be transformed by elementary operations to a set of linear equations of the form

$$z_{n,i} = \rho_{n,i}\phi_{1,i} + \widetilde{\rho}_{n,i}\phi_{2,i}, \quad n = 2, 3, \dots, k,$$
 (17)

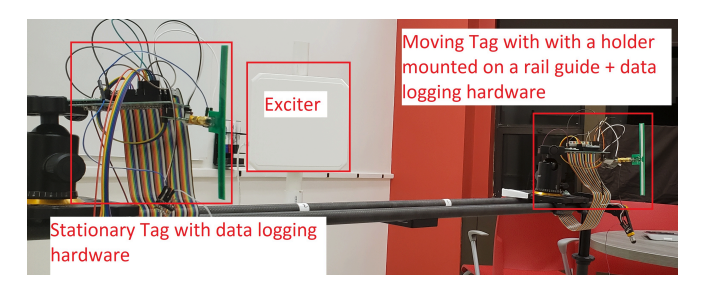


Fig. 3. System overview.

where

$$z_{n,i} = -\frac{\Delta_{n,i}}{2\sin\left(\frac{\varphi_n - \varphi_{n-1}}{2}\right)},$$

$$\rho_{n,i} = \sin\left(\frac{\varphi_n + \varphi_{n-1}}{2}\right), \quad \widetilde{\rho}_{n,i} = \cos\left(\frac{\varphi_n + \varphi_{n-1}}{2}\right),$$

$$\phi_{1,i} = \beta_i \cos \gamma_i, \quad \phi_{2,i} = \beta_i \sin \gamma_i,$$

where the $z_{n,i}s$, $\rho_{n,i}s$, and $\widetilde{\rho}_{n,i}s$ are all known. The system of equations (17) is linear, and the tag can readily obtain the estimates of the unknown parameters $\phi_{1,i}$ and $\phi_{2,i}$. Once these parameters are estimated, the unknown γ_i can easily be obtained from them. We note that with the above approach, the tags do not have to use phases that are uniformly separated.

3. EXPERIMENTAL EVALUATIONS

For experimental demonstration, a prototype RF tag has been designed and fabricated. This tag has a multi-phase modulator and demodulator, which is a passive envelope detector. The tag connects to a custom made dipole antenna tuned to 915 MHz, which is in the middle of the UHF ISM spectrum. The modulator comprises an RF switch that connects one of the k phases to the antenna The selection logic is implemented on a low-power microcontroller stm32f205ret. The impedances are preselected to provide specific reflection phases. The phase values almost uniformly cover the range from 0 to 360 degrees. In the demodulator design, the output voltage of the envelope detector is recorded using a 16 bit ADC which can sample at a rate of 860 samples per second. Figure 2 shows the prototype of the tags.

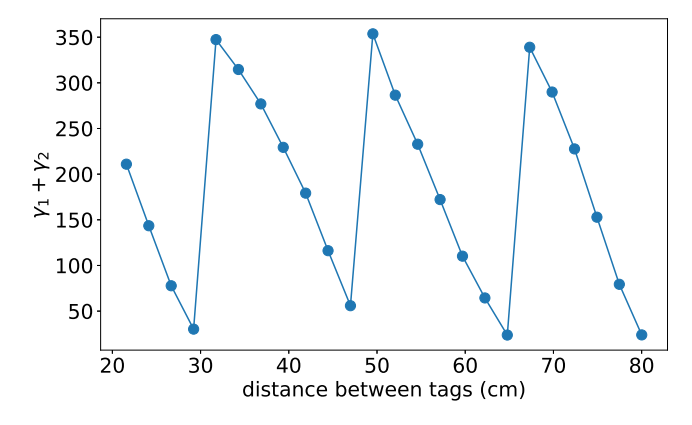


Fig. 4. Change of the channel phase with distance.

We used a CW generator at 915 MHz connected to a circularly polarized panel antenna as excitation source. The exciter is set to a

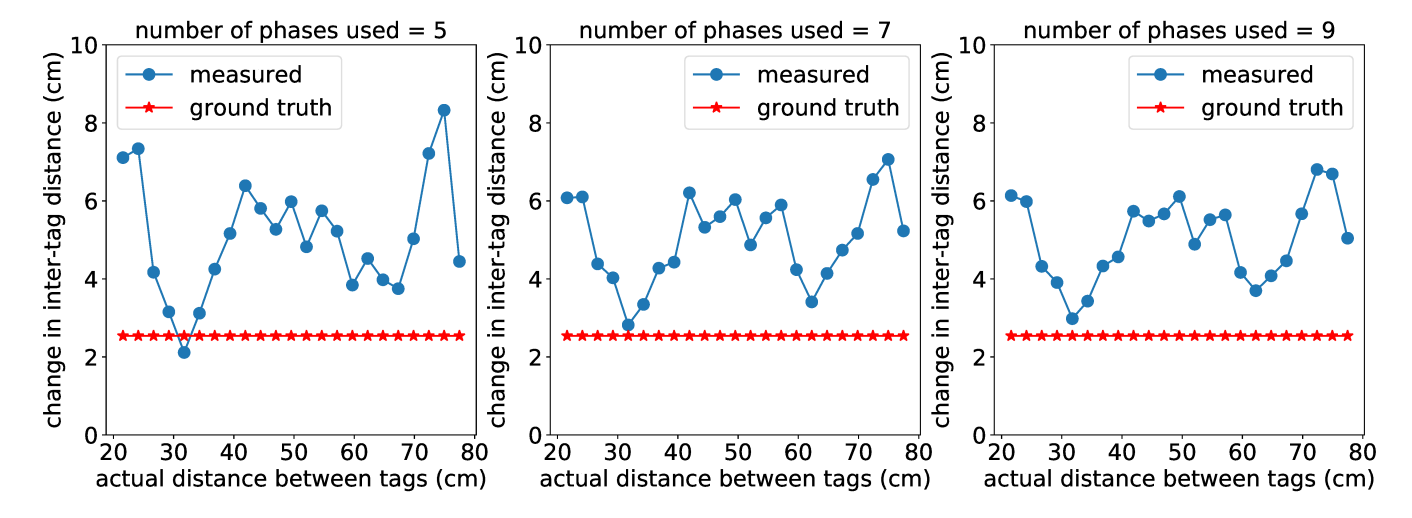


Fig. 5. Tracking accuracy of the tags.

power level of 13 dBm at 1 m to 3 m away from the tags. During the experiments, the data were collected for tag-to-tag distances of 30 to 86 cm. We setup the experiment in an office environment where the exciter and one of the tags remained stationary. The second tag was moved so as to change the inter tag distance. The phase of the phasors θ_{τ} would no longer be constant but would have a rate of change that corresponds to the Doppler shift. In Fig. 4 we plotted $\gamma = \gamma_1 + \gamma_2$ on the ordinate and the distance between the tags on the abscissa. We see that as the distance between the tags changes linearly, the phase drops linearly with a wrapping effect. The rate of change of these values directly corresponds to the relative velocity of the tags.

Next, we show results that correspond to tracking performance. In Fig. 5, the horizontal axis represents the inter-tag distance and the vertical axis is the measured and ground truth change in inter-tag distance. Each plot is for a different number of phases available to the tags. We see that the error for each change in distance is around 0 to 7 cm. We reiterate that the size of the error here is similar to that of a system that uses a conventional active RFID reader [8, 9]. Fig. 6 shows the median error of measuring the inter-tag distance vs the number of phase values available to the tag.

4. DISCUSSION

We recall that one of the biggest challenges in backscatter-based communication is the asymmetry of the channels between the tags. These channels are highly dependent on the position of the exciter. Using our technique we overcome the challenge presented by the asymmetry. Our derivation shows that the phase between two tags is independent of the channels between the exciter and the tags. This implies that during tracking, the relative position of the tags with respect to the exciter is irrelevant for as long as the backscattered signals of the tags are strong enough for maintaining communication.

In related works to ours, authors use anchor nodes as RFID readers. Clearly, the higher the number of used anchor nodes is, the better the accuracy of the estimates would be. However, our method will benefit from anchor nodes much more than the schemes with RFID readers because we can afford to deploy a large number of tags due to their very low cost. Thus, from a network level perspective, we

expect that our scheme would potentially perform better then that with RFID readers. In our future work we will study the accuracy of the estimates as a function of anchor density.

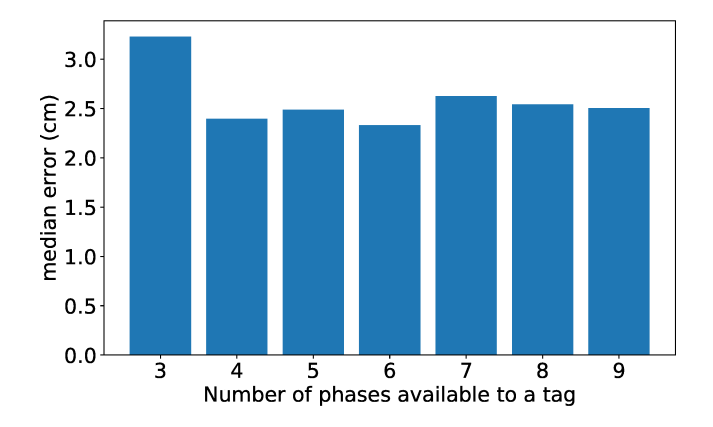


Fig. 6. The median of the error as a function of the number of phases used by the tags.

From Fig. 5 it is apparent that there is a bias in all the measurements. We believe that the bias is a result of an inaccurate hardware calibration. It is, however, interesting to note that other related papers that use phase-based techniques for tracking have biases as well.

5. CONCLUSIONS

In this paper we introduced a technique to measure Doppler shifts by passive tags without requiring an expensive RFID reader. We experimentally evaluated the performance of estimating changes in distances between two tags per unit time. We found that the estimation errors are of the same order as that achieved by an active RFID reader. This suggests that the tracking of objects that are part of the IOT can become scalable. Further, the tracking can be improved if a large network uses many anchor tags with known locations. Such networks will become a reality because the tags they are comprised of will be passive and with very low cost.

6. REFERENCES

- [1] Mohamed Ben-Daya, Elkafi Hassini, and Zied Bahroun, "Internet of things and supply chain management: a literature review," *International Journal of Production Research*, vol. 57, no. 15-16, pp. 4719–4742, 2019.
- [2] Suvendu Naskar, Preetam Basu, and Anup K Sen, "A literature review of the emerging field of iot using rfid and its applications in supply chain management," in Securing the Internet of Things: Concepts, Methodologies, Tools, and Applications, pp. 1664–1689. IGI Global, 2020.
- [3] Klaus Finkenzeller, RFID handbook: Fundamentals and Applications in Contactless Smart Xards, Radio Frequency Identification and Near-field Communication, John Wiley & Sons, 2010.
- [4] Daniel M Dobkin, The RF in RFID: UHF RFID in Practice, Newnes, 2012.
- [5] Yasha Karimi, Akshay Athalye, Samir R. Das, Petar M. Djurić, and Milutin Stanaćević, "Design of a backscatter-based tag-totag system," in *Proceedings of the IEEE International Confer*ence on RFID (RFID), 2017.
- [6] Milutin Stanaćević, Yasha Karimi, Guanchao Feng, Jihoon Ryoo, Akshay Athalye, Samir R Das, and Petar M. Djurić, "RF-based analytics generated by tag-to-tag networks," in ICASSP 2019-2019 IEEE International Conference on Acoustics, Speech and Signal Processing (ICASSP). IEEE, 2019, pp. 8404–8408.
- [7] Jihoon Ryoo, Yasha Karimi, Akshay Athalye, Milutin Stanaćević, Samir R Das, and Petar M. Djurić, "Barnet: Towards activity recognition using passive backscattering tag-totag network," in *Proceedings of the 16th Annual International Conference on Mobile Systems, Applications, and Services*. ACM, 2018, pp. 414–427.

- [8] Lei Yang, Yekui Chen, Xiang-Yang Li, Chaowei Xiao, Mo Li, and Yunhao Liu, "Tagoram: Real-time tracking of mobile rfid tags to high precision using cots devices," in *Proceedings of the 20th Annual International Conference on Mobile Computing and Networking*, New York, NY, USA, 2014, MobiCom '14, pp. 237–248, ACM.
- [9] Yunfei Ma, Nicholas Selby, and Fadel Adib, "Minding the billions: Ultra-wideband localization for deployed rfid tags," in *Proceedings of the 23rd Annual International Conference* on Mobile Computing and Networking, New York, NY, USA, 2017, MobiCom '17, pp. 248–260, ACM.
- [10] Jue Wang, Deepak Vasisht, and Dina Katabi, "Rf-idraw: Virtual touch screen in the air using rf signals," SIGCOMM Comput. Commun. Rev., vol. 44, no. 4, pp. 235–246, Aug. 2014.
- [11] Jinsong Han, Chen Qian, Dan Ma, Xing Wang, Jizhong Zhao, Pengfeng Zhang, Wei Xi, and Zhiping Jiang, "Twins:devicefree object tracking using passive tags," 2013.
- [12] Fu Xiao, Zhongqin Wang, Ning Ye, Ruchuan Wang, and Xiang-Yang Li, "One more tag enables fine-grained rfid localization and tracking," *IEEE/ACM Trans. Netw.*, vol. 26, no. 1, pp. 161–174, Feb. 2018.
- [13] Pat Pannuto, Benjamin Kempke, and Prabal Dutta, "Slocalization: Sub-w ultra wideband backscatter localization," in Proceedings of the 17th ACM/IEEE International Conference on Information Processing in Sensor Networks, Piscataway, NJ, USA, 2018, IPSN '18, pp. 242–253, IEEE Press.
- [14] Lei Yang, Jiannong Cao, Weiping Zhu, and Shaojie Tang, "Accurate and efficient object tracking based on passive rfid," *IEEE Transactions on Mobile Computing*, vol. 14, no. 11, pp. 2188–2200, Nov. 2015.

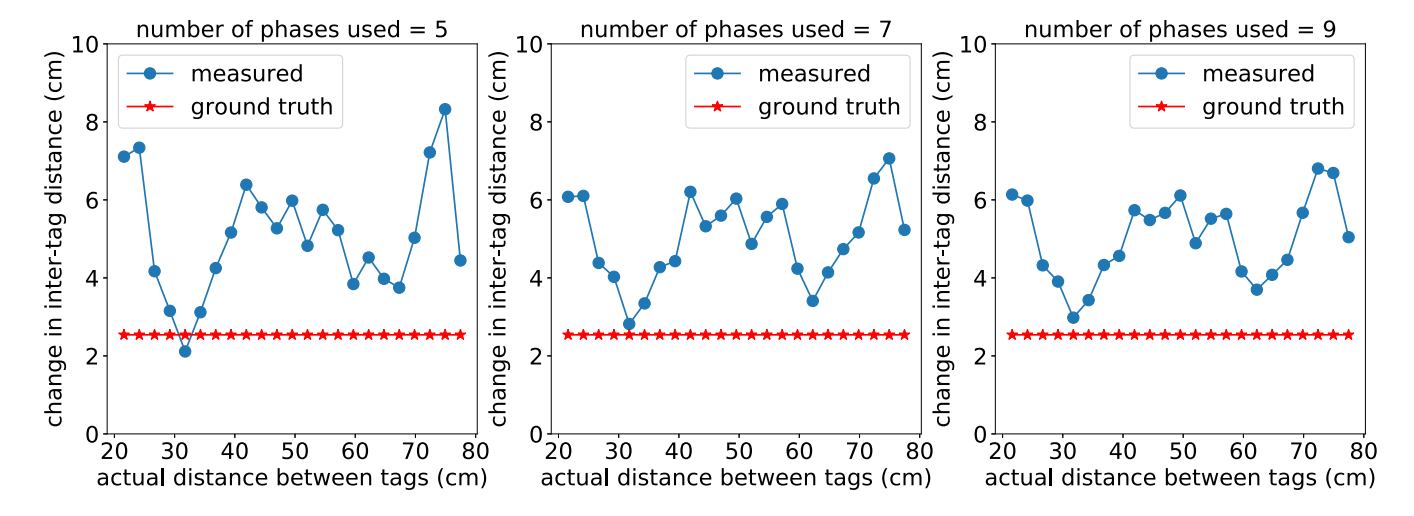


Fig. 5. Tracking accuracy of the tags.

power level of 13 dBm at 1 m to 3 m away from the tags. During the experiments, the data were collected for tag-to-tag distances of 30 to 86 cm. We setup the experiment in an office environment where the exciter and one of the tags remained stationary. The second tag was moved so as to change the inter tag distance. The phase of the phasors θ_τ would no longer be constant but would have a rate of change that corresponds to the Doppler shift. In Fig. 4 we plotted $\gamma=\gamma_1+\gamma_2$ on the ordinate and the distance between the tags on the abscissa. We see that as the distance between the tags changes linearly, the phase drops linearly with a wrapping effect. The rate of change of these values directly corresponds to the relative velocity of the tags.

Next, we show results that correspond to tracking performance. In Fig. 5, the horizontal axis represents the inter-tag distance and the vertical axis is the measured and ground truth change in inter-tag distance. Each plot is for a different number of phases available to the tags. We see that the error for each change in distance is around 0 to 7 cm. We reiterate that the size of the error here is similar to that of a system that uses a conventional active RFID reader [8, 9]. Fig. 6 shows the median error of measuring the inter-tag distance vs the number of phase values available to the tag.

4. DISCUSSION

We recall that one of the biggest challenges in backscatter-based communication is the asymmetry of the channels between the tags. These channels are highly dependent on the position of the exciter. Using our technique we overcome the challenge presented by the asymmetry. Our derivation shows that the phase between two tags is independent of the channels between the exciter and the tags. This implies that during tracking, the relative position of the tags with respect to the exciter is irrelevant for as long as the backscattered signals of the tags are strong enough for maintaining communication.

In related works to ours, authors use anchor nodes as RFID readers. Clearly, the higher the number of used anchor nodes is, the better the accuracy of the estimates would be. However, our method will benefit from anchor nodes much more than the schemes with RFID readers because we can afford to deploy a large number of tags due to their very low cost. Thus, from a network level perspective, we

expect that our scheme would potentially perform better then that with RFID readers. In our future work we will study the accuracy of the estimates as a function of anchor density.

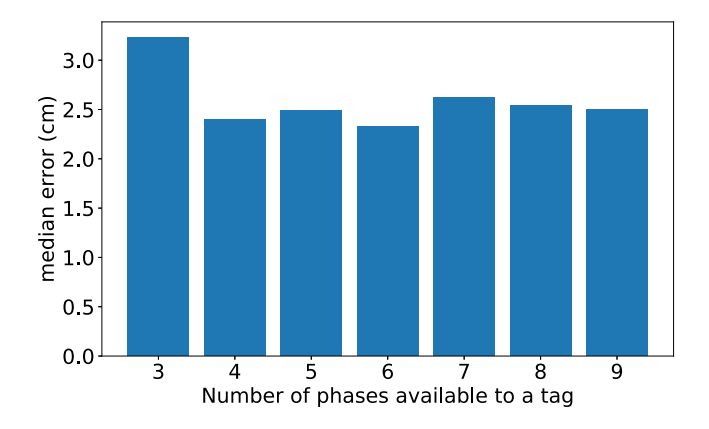


Fig. 6. The median of the error as a function of the number of phases used by the tags.

From Fig. 5 it is apparent that there is a bias in all the measurements. We believe that the bias is a result of an inaccurate hardware calibration. It is, however, interesting to note that other related papers that use phase-based techniques for tracking have biases as well.

5. CONCLUSIONS

In this paper we introduced a technique to measure Doppler shifts by passive tags without requiring an expensive RFID reader. We experimentally evaluated the performance of estimating changes in distances between two tags per unit time. We found that the estimation errors are of the same order as that achieved by an active RFID reader. This suggests that the tracking of objects that are part of the IOT can become scalable. Further, the tracking can be improved if a large network uses many anchor tags with known locations. Such networks will become a reality because the tags they are comprised of will be passive and with very low cost.